Changes in event-related potential functional networks predict traumatic brain injury in piglets

Clinical Biomechanics 64 (2019) 14–21

Contents lists available at ScienceDirect

Clinical Biomechanics

journal homepage: www.elsevier.com/locate/clinbiomech

Changes in event-related potential functional networks predict traumatic brain injury in piglets

Lorre S. Atlan[a], Ingrid S. Lan[a], Colin Smith[b], Susan S. Margulies[a,*]

[a] Department of Bioengineering, University of Pennsylvania, 210 S. 33rd St., 240 Skirkanich Hall, Philadelphia, PA 19104-6321, USA
[b] Academic Department of Neuropathology, Centre for Clinical Brain Sciences, University of Edinburgh, Edinburgh, UK

ARTICLE INFO

Keywords:
Auditory
Event-related
Functional
Networks
Traumatic brain injury
Pediatric

ABSTRACT

Background: Traumatic brain injury is a leading cause of cognitive and behavioral deficits in children in the US each year. None of the current diagnostic tools, such as quantitative cognitive and balance tests, have been validated to identify mild traumatic brain injury in infants, adults and animals. In this preliminary study, we report a novel, quantitative tool that has the potential to quickly and reliably diagnose traumatic brain injury and which can track the state of the brain during recovery across multiple ages and species.

Methods: Using 32 scalp electrodes, we recorded involuntary auditory event-related potentials from 22 awake four-week-old piglets one day before and one, four, and seven days after two different injury types (diffuse and focal) or sham. From these recordings, we generated event-related potential functional networks and assessed whether the patterns of the observed changes in these networks could distinguish brain-injured piglets from non-injured.

Findings: Piglet brains exhibited significant changes after injury, as evaluated by five network metrics. The injury prediction algorithm developed from our analysis of the changes in the event-related potentials functional networks ultimately produced a tool with 82% predictive accuracy.

Interpretation: This novel approach is the first application of auditory event-related potential functional networks to the prediction of traumatic brain injury. The resulting tool is a robust, objective and predictive method that offers promise for detecting mild traumatic brain injury, in particular because collecting event-related potentials data is noninvasive and inexpensive.

1. Introduction

Traumatic brain injury (TBI) can be defined as alterations in brain function resulting from an external force (Eucker et al., 2011). TBI is the leading cause of disability and death in children in the United States and the two age groups that are at highest risk for TBI are infants and toddlers (0–4 years) and young adults (15–19 years) (Faul et al., 2010). Given the significant cost and impact of mild pediatric TBI in the US, there is an urgent need for accurate diagnostic tools to identify mild TBI in the young brain.

Currently, there are no biomarkers available for the diagnosis and prognosis of concussion in children (Davis et al., 2017). Clinicians typically use balance or eye-tracking and cognitive tests; however, there is little data to support their use to assess concussion in children aged 5–12 years (Davis et al., 2017). A multimodal framework that enables age-appropriate diagnosis and clinical assessment of pediatric concussion as well as prognosis of recovery is necessary.

Event-related potentials (ERPs) are electrical signals evoked in response to a sensory stimulus. ERPs consist of characteristic sequences of peaks and troughs called ERP components that indicate cognitive processing. Auditory ERPs, evoked in response to an auditory stimulus, are involuntary, do not require prior training of the subject and permit easy control of the stimuli. Several studies show persistent changes in the amplitudes and latencies of auditory ERP components in TBI patients compared to controls (De Beaumont et al., 2007; Dundon et al., 2015; Mazzini et al., 2001). In this study, we recorded auditory ERPs in juvenile piglets to develop quantitative, unbiased predictors of brain state after injury.

Traditionally, the analysis of ERPs is component-dependent, where researchers infer the significance of the changes in the magnitude and latency of the ERP components from different channels located in regions associated with specific cognitive processing states in humans. However, such an analysis of ERP components is subjective. Network analysis allows simultaneous investigation of neural activity recorded by all the electrodes, thereby eliminating component- and method-specific bias. In this preliminary study, we generated functional

* Corresponding author at: Georgia Tech, The U.A. Whitaker Biomedical Engineering Building, 313 Ferst Drive, Atlanta, GA 30332-0535, USA.
E-mail addresses: latlan@seas.upenn.edu (L.S. Atlan), ingridl@seas.upenn.edu (I.S. Lan), Col.Smith@ed.ac.uk (C. Smith), susan.margulies@gatech.edu (S.S. Margulies).

https://doi.org/10.1016/j.clinbiomech.2018.05.013
Received 30 November 2017; Received in revised form 19 April 2018; Accepted 21 May 2018

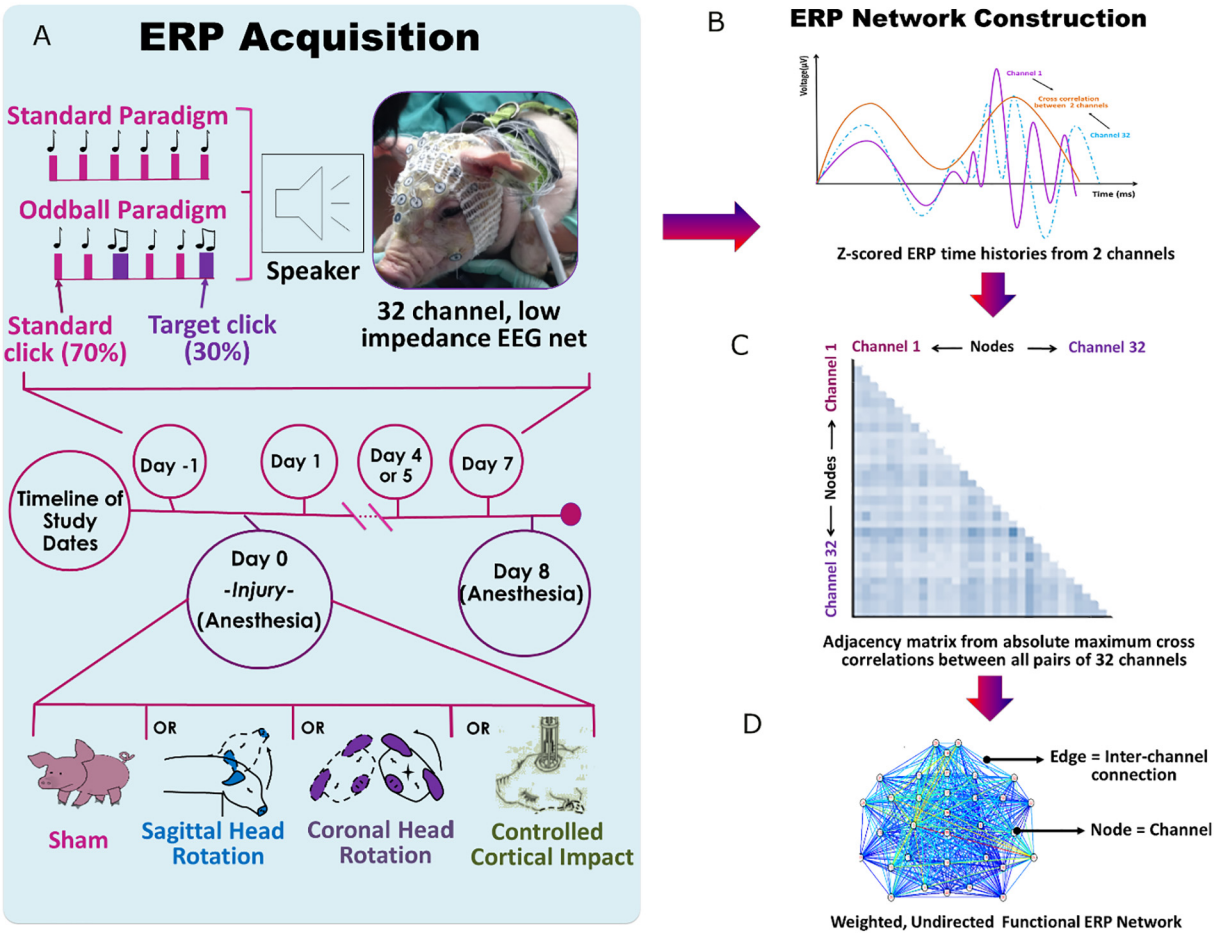

Fig. 1. Schematic describing auditory ERP acquisition and functional network construction methods.

networks before and after well-characterized diffuse and localized white matter injury in piglets to evaluate whether significant alterations occur in post-TBI ERPs.

2. Materials and methods

2.1. Diffuse & localized injury in piglets

All animal experimental protocols were approved by the Institutional Animal Care and Use Committee (IACUC) of the University of Pennsylvania. Twenty-two 4-week-old female Yorkshire piglets were used, equivalent to the human toddler (Dickerson and Dobbing, 1967).

Piglets were allocated to an injury or sham group. All piglets were anesthetized with 1.5% isoflurane, intubated and mechanically ventilated. Either a focal injury via controlled cortical impact (CCI) or a diffuse injury by rapid non-impact sagittal rotation (RNR) (Margulies et al., 2015) was prescribed to the piglets in the injury group. Sagittal RNRs at approximately 130 rad/s were prescribed and previously determined to induce mild TBI (Margulies et al., 2015; Weeks et al., 2014). ERPs were measured one day before injury and on 1, 4, and 7 days after injury. Sample sizes for each group of piglets in this preliminary study were 9 for Sham, 7 for sagittal (SAG) RNR, 3 for coronal (COR) RNR and 3 for CCI.

2.2. Immunohistochemistry

Immunohistochemical processing of a sub-sample of piglet brains was performed 8 days after injury. Brains were perfused and fixed with 10% neutral buffered formalin for 24 h (Ibrahim et al., 2010). Sections were stained for beta-amyloid precursor protein. Positive staining, indicative of damaged axons, was identified by a neuropathologist blind to the injury group. The cumulative sum of positively stained area was used to calculate an axonal injury volume (AIV), calculated as a percent of total cerebral volume.

2.3. Data acquisition and auditory stimulus

The E-Prime (2.0.10.353 SPI) software program, a 32-channel net (Electrical Geodesics, Inc. HydroCel™ Geodesic Sensor Net) and Electrical Geodesics, Inc. Net Amps 400 EEG amplifier were used to generate auditory stimuli and acquire neural responses.

Two sequences of 100 2-ms clicks were played by a portable USB speaker to each piglet for the standard (Std) and oddball (OB) paradigms. The clicks in the standard paradigm were “white noise”, at 800 Hz auditory frequency. Clicks in the OB paradigm consisted of a random combination of 70% standard (OB-Std) “white noise” clicks (same as used in the Std paradigm) and 30% target (OB-Trgt) “brown noise” clicks (auditory frequency of 1000 Hz). Paradigms were repeated until a minimum of two acceptable standard trains and oddball trains per piglet were obtained.

2.4. Traditional analysis of ERP amplitudes and latencies for selected channels

Amplitudes and latencies of ERP components were detected using a custom MATLAB® (R2015b, Mathworks, Inc.) script. Four distinct ERP components identified from previous studies in adult pigs were selected for analysis. The first two peaks and troughs in the ERP signals from

channels 15 (left auditory cortex), 16 (right auditory cortex), 17 (near frontal lobe midline), 19 (parietal lobe midline), 20 (occipital lobe midline), and 28 (near central midline) were selected because they are conventionally studied in the ERP literature (Andrews et al., 1990; Arnfred et al., 2004; Heisz and McIntosh, 2013; Martoft et al., 2001; Rogers et al., 2015). The latency ranges for each peak were based on the information from a study performed in adult Gottingen mini-pigs (Arnfred et al., 2004). The four ERP components examined were: N40 (the negative peak found in the latency range of 20–60 ms post-stimulus), P60 (positive peak found in range of 40–80 ms), N120 (negative peak found in range of 90–150 ms) and P200 (positive peak found in range of 150–250 ms). If a peak with the correct polarity was not found in the specified latency range of the ERP for a specified channel, the peak was excluded from analysis.

2.5. Generation of auditory ERP functional networks

A single network edge between two channels was constructed by calculating the maximum absolute cross-correlation between the averaged, z-scored post-stimulus ERP signals from both channels (Fig. 1B). The collection of cross-correlations between all pairs of channels form the network, which is depicted as a 32 × 32 matrix (Fig. 1C) and a set of connections between electrode sensor locations (Fig. 1D).

Our ERP networks were fully connected with a network density of 1 defined as 496 edges among 32 nodes. ERP networks, as a function of network density, were generated by progressively removing the weakest edges. In order to threshold each network, network edges with values below the range of 48th–99th percentile edge values were sequentially removed. The range of thresholds was applied to each network and subsequently a series of network metrics on each thresholded network were calculated in order to examine the effect of density on sham, SAG, COR and CCI networks.

We calculated two network metrics on the thresholded networks in order to quantify functional network influence, integration and segregation in the brain: nodal strength and global efficiency. Nodal strength (NS) was calculated as the sum of all connections or edges from a specified node. Paths are unique sequences of edges between two distinct nodes and their lengths are measured by the sum of edges. Global efficiency (GE) was calculated as the average of the inverse of the shortest path lengths in the network.

2.6. Discrimination of injured and uninjured ERPs

Each post-click signal was classified as injured or not injured. There were three types of epochs (and data sets): Standard (Std), Oddball-Standard (OB-Std) and Oddball-Target (OB-Trgt). A single machine learning model was constructed for each type of epoch. Preprocessed ERP signals were used to construct the model.

To construct our machine learning models, a binary classification dataset was created, in which epochs were classified as uninjured if they were acquired before injury (Day 0) in the SAG and CCI groups. Sham epochs from all days were also classified as uninjured. ERP epochs were classified as injured if acquired between 1 and 5 days after injury in the SAG and CCI groups. The data set was randomly split into three sets: training (38%), testing (38%) and validation (24%). The training set was used to tune the parameters of the model, the testing set was used to select the final model and the validation set was used to report the predictive capability of the model with metrics such as accuracy and area under ROC curve (AUC). All performance data presented in this report were determined from the validation set. CORs were not included in our training set because it is characteristically a mild TBI (in terms of total axonal injury volume) compared to CCI and SAG (Eucker et al., 2011; Ibrahim et al., 2010). Instead, we evaluated the performance of CORs using the algorithm separately.

To improve the accuracy of the predictive model, the ERP data were dimensionally reduced using XDawn, a novel dimensionality reduction algorithm that is similar to principal component analysis, which maximizes signal-to-noise ratio of ERPs (Barachant et al., 2012; Rivet, 2009.; Rivet and Souloumiac, 2007) and outputs data with a reduced number of components in the channel dimension. The dimensionally reduced ERP data were then used to calculate covariance matrices for each ERP epoch using XDawnCovariance (XDawnCov); this step simplifies classification of data into injured and uninjured groups. To predict TBI, the output from a separate logistic regression model (Pedregosa et al., 2011) applied to Xdawn and XDawnCov was averaged and a single predictive model for each ERP paradigm was constructed.

Each predictive model outputs two scores representing the probabilities that an epoch belongs to the injured and uninjured class, where the sum of both scores for the same epoch is 1. For each animal, a probability score for injury (InjScore) was computed as the geometric mean (over the range of 0 to 1) of probability scores for the injured class for all ERP epochs. In order to convert the continuous InjScore to a discrete classification (injured or uninjured), we applied the k-means clustering (Pedregosa et al., 2011) method (k = 2) to each paradigm's InjScores. All three paradigms were combined by taking the majority vote over all discrete InjScore classifications for every animal. We also analyzed the mean of all continuous InjScores from each paradigm for each animal. An ROC analysis was used to determine the critical value of InjScore above which animals should be classified injured. The InjScore threshold was taken where both the true positive rate was highest and the false positive rate was lowest.

2.7. Statistical analyses

The non-parametric Dunnett's test (Gao, 2008) was used for comparison of ERP latencies and magnitudes between Day-1 (PRE) and all post-injury days (POST 1 d, 4 d and 7 d). For the analysis of network metrics as a function of network density, group differences between SAG, COR and CCI compared to Sham were found by performing two-tailed permutation tests at each density value and then correcting for multiple comparisons using the Benjamini-Hochberg correction procedure (Harris et al., 2016). The level of significance was 0.05 for all statistical tests. All statistical tests were performed in R 3.4.1 (R Core Team, 2017).

3. Results

3.1. Histopathology

Histopathological assessment of axonal damage yielded a mean of 0.0% in Sham (n = 3), 0.31% of total cerebral volume in SAG (n = 2), 0.0% in COR (n = 3) and 4.69% in CCI (n = 1) animals respectively, similar to our previous findings (Eucker et al., 2011; Margulies et al., 2015). Based on axonal histopathology, we expected that COR would present mild alterations in ERPs compared to SAG and CCI to be consistent with lower axonal injury damage.

3.2. Traditional analysis of ERP amplitudes and latencies for selected channels

The median values of the amplitudes and latencies of the N40, P60, N120 and P200 components from channels 15, 16, 17, 19, 20, and 28 were largely unchanged from PRE levels and did not vary widely in response to SAG injury or study day (Fig. 2). For N40 latencies, the POST 7 d time point only the SAG group was significantly longer (non-parametric Dunnetts test, $p = 0.01$) than PRE for Channel 15. All other comparisons of N40 latencies and amplitudes from post-injury to pre-injury for channels 15, 16, 17, 19, 20, and 28 were not significantly different ($p > 0.05$). Channel 19's P60 amplitudes decreased significantly on all post-SAG days relative to PRE. A reduction in P60 amplitudes at 4d was only seen in the Sham group compared to PRE (Fig. 2). All significant changes in the latencies and amplitudes of N120

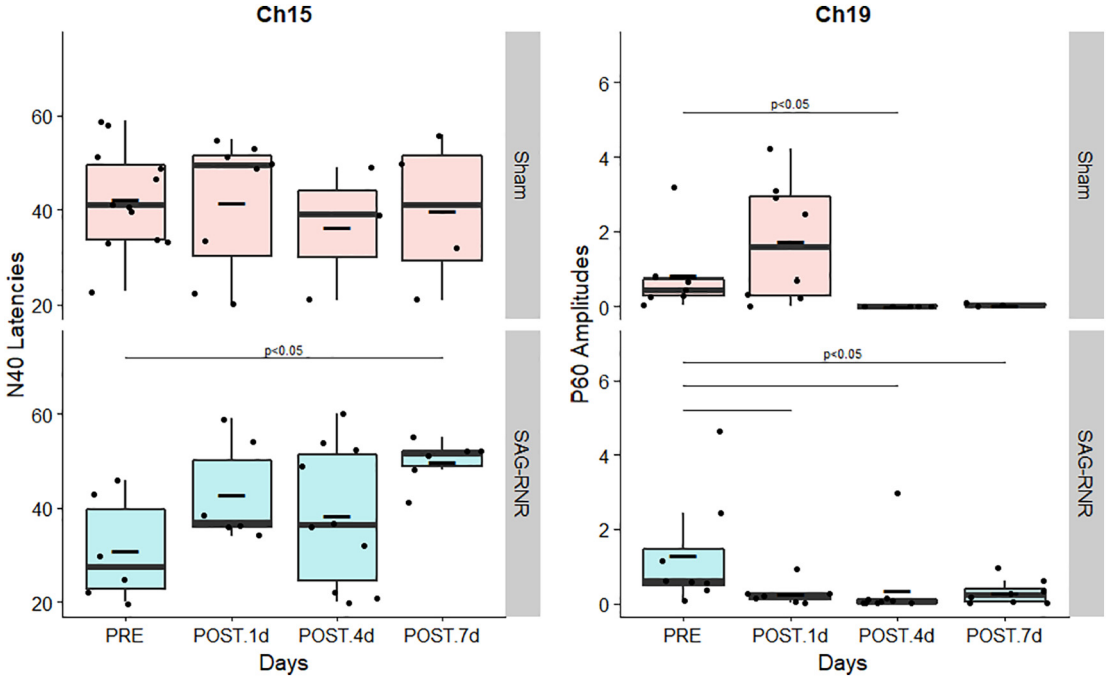

Fig. 2. Median N40 latencies for channel 15 (left auditory cortex) and P60 amplitudes for channel 19 (parietal lobe midline) in Sham and SAG groups from the Standard paradigm.

or P200 in the SAG group were also present in the Shams, from channels 16, 17, 20 and 28. In summary, significant changes in amplitudes and latencies from PRE levels were observed in early peaks (N40 and P60) in the SAG group. For the traditional ERP analysis, statistical tests were not performed on data from COR and CCI because of small sample sizes (n = 3).

3.3. TBI alters auditory ERP networks

We thresholded our networks to remove weak edges as removal of weak edges in the network reveals the largest differences in network properties between the sham and injured groups that may not be evident at a single network density value. Nodal strength (NS) quantifies the number and strength of the connection that each electrode has to all other electrodes, where a higher nodal strength represents increased synchrony with ERPs from other electrodes. NS increased as network density increased because more edges implies a greater sum of connections. Before injury, all NS curves from injury groups were not significantly different ($p > 0.28$) from sham (Fig. 3). At POST 1 d, there was a large reduction in NS values ($p < 0.012$) in all injury groups by 31.9% (in SAG), 34.4% (in COR) and 43.4% (in CCI) relative to Sham. This suggests that local connectivity decreased 1d after all modes of injury relative to Sham. By POST 4 d, NS of COR and CCI injury groups increased ($p < 0.03$) relative to Sham, and by POST 7 d all injury groups' NS values were comparable to Sham ($p > 0.2$). By POST 7 d, NS values from Sham, SAG, COR and CCI have magnitudes comparable to PRE NS values.

Global Efficiency (GE) quantifies functional integration, which is the ability to combine specialized information from distributed brain regions. GE estimates the ease with which brain regions communicate, and is commonly based on the concept of a path. As more network edges are added to a network and network density increases, GE in turn increases (Fig. 4). GE values were significantly different ($p < 0.05$) on PRE for the COR and SAG groups compared to Sham, but not for CCI. All GE values were similar to sham at POST 1 d for all injury groups ($p > 0.14$). On POST 4 d, SAG, COR and CCI showed lower GE values ($p < 0.02$) than Sham at network density of 1. SAG, CCI, and COR injuries also showed lower ($p < 0.049$) GE values at POST 7 d compared to Sham at network densities > 0.75. A higher global efficiency implies stronger connectivity or information transfer between the two most weakly connected nodes in the network.

3.4. Discrimination between injured and uninjured ERPs

Our objective was to develop a robust metric for identifying TBI in a given animal using our ERP dataset. The Std predictive algorithm outperforms both OB Std and OB Trgt, which indicates that the Std paradigm may be the most informative individual paradigm for predicting injury. However, we obtained maximal predictive performance (82% accuracy, AUC = 0.82), when we combined the output of all three paradigms (Table 1).

The mean InjScore from all paradigms for each injury group (Sham, SAG, COR or CCI) on days-1, 1 or 4 was calculated (Fig. 5). Sham/Pre-injury had the lowest mean InjScore (0.14), compared to the remainder of injury groups and days, while SAG at day 4 had the largest mean InjScore value (0.32), indicating a higher number of composite ERP epochs that were predicted to be injured. The mean InjScores for SAG at days 1 ($p = 0.022$) and 4 ($p = 0.02$) were significantly larger than that for Sham/Pre-injury. All post-CCI comparisons were not significantly different ($p > 0.19$) from Sham/Pre-injury. The ROC analysis of InjScores against their true classifications revealed InjScores thresholds as 0.13 (Sensitivity: 55%, Specificity: 92%) for Std, 0.18 (Sensitivity: 54%, Specificity: 75%) for OB-Std, 0.19 (Sensitivity: 64%, Specificity: 75%) for OB-Trgt and 0.18 (Sensitivity: 54%, Specificity: 75%) for all paradigms. Although the InjScore may range from zero to one, InjScores from the combination of all paradigms that exceeded 0.19 were associated with being classified as injured.

Using our validation set, eight out of nine Sham or pre-injured animals were correctly predicted as uninjured. All CCI animals (n = 2) were classified as having uninjured auditory ERPs on post-injury day 1, and an injured ERP signature on post-injury day 4. All SAG animals were classified as injured on both post-injury days 1 and 4 (n = 2 each).

The mean InjScore for day 1 post-COR animals was not significantly different ($p = 0.29$) from that of the uninjured group. Only one out of three COR animals was classified as injured on day 1 compared with 100% of SAG and 0% of CCI. The “uninjured” classification of animals

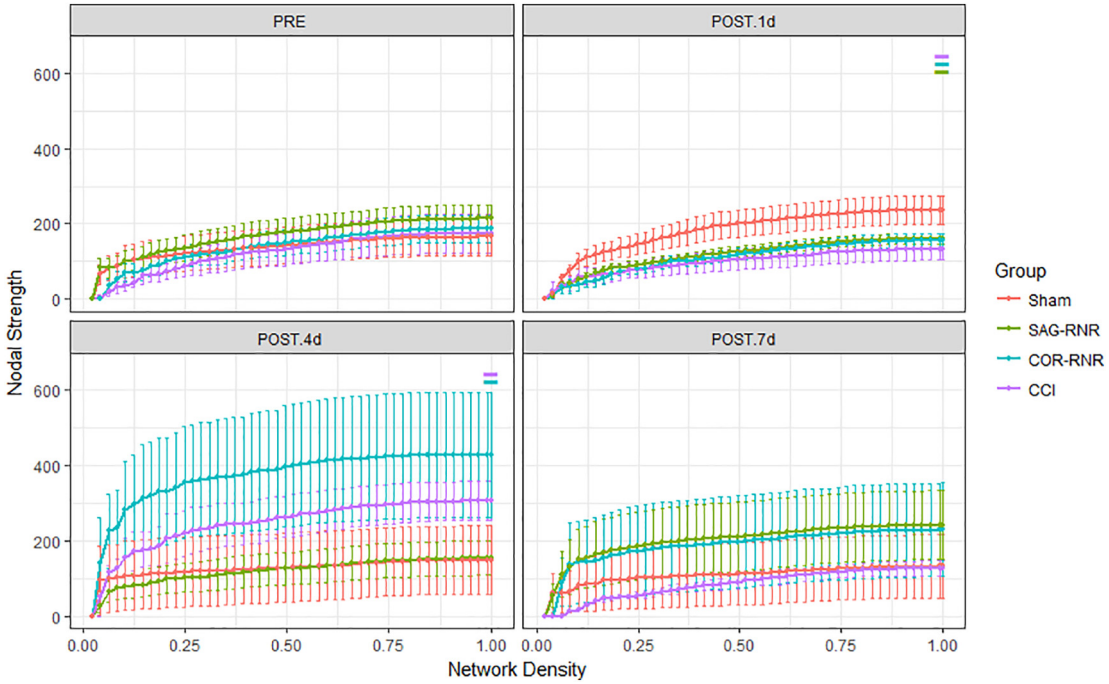

Fig. 3. Changes in nodal strength with network density for all injury groups and study dates compared to Sham from Standard paradigm. Mean values and standard error bars are shown. Horizontal bars indicate significant difference of injury groups from sham at single density level using two-tailed permutation test with false detection rate correction for multiple comparisons, $p < 0.05$.

experiencing rapid head rotations in COR was consistent with our finding of reduced axonal injury in COR. We also find no significant alterations in auditory ERPs at 1 day after a rapid COR head rotation.

4. Discussion

Auditory ERP components represent auditory information processing (Gosselin et al., 2006), which involves the sensory and limbic systems. ERPs provide the advantages of high temporal resolution, non-invasive and inexpensive recording of brain activity compared to CSF or blood-based biomarkers, DTI and fMRI. At the time of this publication, there are no studies that used auditory ERP networks to predict pediatric TBI.

Based on previous ERP studies (De Beaumont et al., 2007; Dennis et al., 2015; Dundon et al., 2015; Mazzini et al., 2001) conducted in humans, we expected TBI to cause smaller peak amplitudes and longer

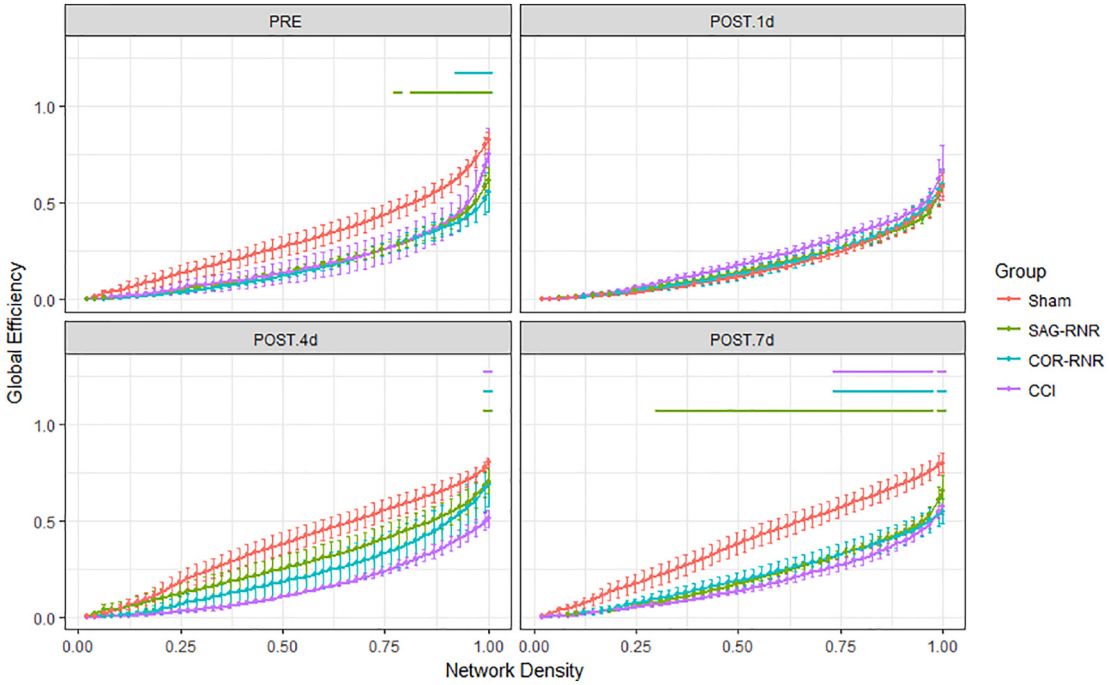

Fig. 4. Changes in global efficiency with network density for all injury groups and study dates compared to Sham from Standard paradigm. Mean values and standard error bars are shown. Horizontal bars indicate signficant difference of injury groups from sham at density level using two-tailed permutation test with false detection rate correction for multiple comparisons, $p < 0.05$.

Table 1
Accuracy, area under ROC curve and precision of TBI prediction algorithm performed on validation set from Standard, Oddball Standard, Oddball Target and majority vote over all three paradigms.

	Accuracy	AUC	Precision
Standard	76.47	0.75	1.00
OB Standard	47.06	0.49	0.46
OB Target	70.59	0.71	0.67
Majority vote (all)	82.35	0.82	0.86

latencies in the majority of channels, however we only observed this in a few channels in our piglets. Piglet brains provide a platform for better understanding the young child brain due to similar neuroanatomy and development (Buckley, 1986; Dickerson and Dobbing, 1967; Duhaime, 1998; Margulies et al., 2015). While the characterization of auditory ERP components in pigs is not as well developed as it is in humans, this report suggests that knowledge of ERP components may be unnecessary for identification of TBI. Also, previous publications indicate that auditory structures are highly consistent between pigs and humans (Yi et al., 2016).

4.1. Traditional analysis of ERPs poorly discriminated TBI

In our study, the traditional analysis of magnitudes and latencies from auditory ERPs poorly discriminated TBI in piglets. Kraus et al. recently used characteristic auditory brainstem ERPs to accurately predict severity of concussion in children, but did not validate their findings with a separate dataset (Kraus et al., 2016). Our study shows longer latencies and lower amplitudes, with partial recovery compared to the pre-injury baseline in select channels. Network analyses use all the data from all channels as a robust means of gaining insight into the effect of TBI on neural activity that may be relevant to the study of TBI in various species and ages.

4.2. TBI alters auditory ERP networks

Few researchers study pediatric TBI and those that do, use a subject population with highly variable ages, post-injury dates and brain injury types (Dennis et al., 2015; Espy et al., 2004; Kraus et al., 2016). These factors may explain the confounding results reported in human TBI functional network literature. There are very few animal studies of functional networks after TBI.

In rats with focal brain injury, increases in nodal strength and efficiency in resting-state fMRI BOLD networks were reported 7 days after CCI, but not at 14 and 28 days post-injury relative to pre-injury (Harris et al., 2016). We found no change in nodal strength and a decrease in efficiency 7 days after CCI relative to Sham. Harris and colleagues imaged rats under medetomidine sedation and did not include shams, making comparison with our study difficult.

Hypo- and hyperconnectivity varied in our study after injury by injury type and time point. Similarly, several studies have shown conflicting findings on the effect of TBI on functional networks –some proposing hyper-connectivity (Harris et al., 2016; Hillary et al., 2014, 2015; Sharp et al., 2011) and others hypo-connectivity (Kumar et al., 2009; Mishra et al., 2014; Rigon et al., 2015; Stevens et al., 2012). We believe that the discrepancy in the effect of TBI on functional connectivity may be dependent on recovery time, type of stimuli, neuroimaging technique, regions analyzed and heterogeneity of TBI subject population. The axonal damage found in the piglet cerebrum 8 days after TBI may be the cause of acute hypo-connectivity observed, where loss of axonal connectivity causes a failure of synchrony between cortical neurons. However, axonal damage was observed after SAG and CCI injuries, but not in COR. We speculate that the absence of axonal

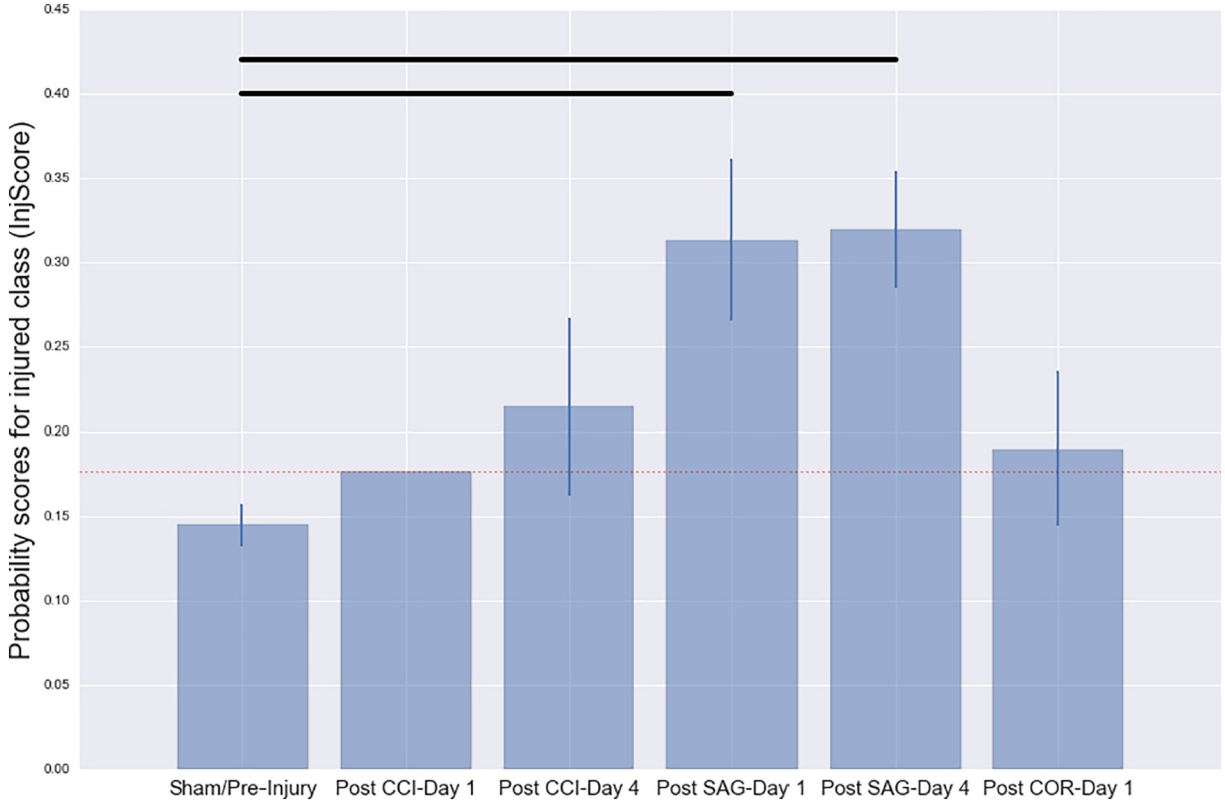

Fig. 5. Mean and standard error bar charts of injury probability scores (InjScores) for all paradigms from XDawn/XDawnCov machine learning models. Black horizontal lines represent significant Wilcoxon ranksum test comparison with Sham/Pre-injury, $p < 0.05$. The red, dotted line represents the threshold of InjScore determined from ROC analysis. (For interpretation of the references to color in this figure legend, the reader is referred to the web version of this article.)

damage after COR may be due to intact but dysfunctional axons. A task-related fMRI study has demonstrated less inter-hemispheric functional connectivity in their TBI cohort, compared with healthy controls (Rigon et al., 2015), which may suggest weakening functional edges in the corpus callosum due to structural damage. Evidence of disrupted functional EEG connectivity in the brain after combat-related blast injury was reported 32 months after blast exposure (Sponheim et al., 2011), which may support our hypothesis of intact but dysfunctional axons.

Hypo-connectivity following TBI may be the result of cellular dysfunction (node failure) or white matter damage (edge failure). White matter degradation may explain the decreased connectivity observed across the ERP networks on day 1 after SAG injury compared to Sham. Recent studies have found that functional connectivity patterns largely reflect that of underlying structural or white matter connectivity (Dennis et al., 2015; Honey et al., 2009; Mayer et al., 2011; Sharp et al., 2011). However, it is unclear how much white matter tract integrity must be disrupted in order to affect functional connectivity, and how global and regional functional connectivity varies as a result. More research is needed to further our understanding of the relationship between the loss of white matter microstructure and functional disconnection.

Several studies have demonstrated that the direction of head motion strongly affects the extent of axonal injury in various animal models and ages (Atlan et al., 2017; Browne et al., 2011; Duhaime et al., 1987; Gennarelli et al., 1982; Smith et al., 2003). By performing rapid head rotations about the SAG and COR planes, we varied TBI severity by modulating the amount of stretching along the white matter tracts in order to examine its effect on functional connectivity. In our neonatal and juvenile pig models, SAG rapid head rotations cause significantly higher magnitudes of AIV compared to COR (Sullivan et al., 2015). The minimum AIV was found at 5–6 day post-injury compared to 3–8 h, 1 day and 3–4 days, maximal AIV of 1.15% was observed at 1 day post-injury in 4-week old piglets (Weeks et al., 2014). The AIV found in this report align with previous reports. CCI had more focal axonal damage than SAG, but larger AIV compared to SAG and COR rapid head rotations. We speculate that any significant change in ERP networks is due to deficits in cognitive ability due to the magnitude and regional location of axonal injury.

4.3. Accurate discrimination between injured and uninjured ERPs

The XDawn and XDawnCov techniques have both been successfully used to discriminate between ERP responses to different visual cues (Barachant et al., 2012; Rivet, 2009, 2011). This study was a novel application of XDawn/XDawnCov technique to the study of TBI. XDawnCov was able to extract insight between injured and uninjured animals by looking at covariance matrices, which similarly capture synchrony across the brain, like the cross-correlation networks previously discussed.

Our injury prediction algorithm, combining Std and OB paradigms, was able to reliably classify injured animals with > 80% accuracy. This study is the first ERP network study on TBI in animals. This EEG-based biomarker may have direct application to humans, including infants, providing clinicians the ability to track recovery states of brain injury in subjects and to quantitatively assess whether a treatment is working appropriately. To summarize, we have developed an auditory EEG-based tool that detects mild TBI after trauma. It is non-invasive, portable, fast and inexpensive compared to other neuroimaging techniques.

Similar to other neuro-imaging modalities, the application of ERPs to the study of TBI has several limitations such as wide variability within and between subjects and sensitivity to subject alertness. Although our findings were statistically significant, our sample size was modest and our findings should be replicated in a larger subject cohort.

5. Conclusions

Network analysis provides an objective, quantitative framework for analyzing multi- source neural signals. We observed functional connectivity alterations in auditory ERP networks due to diffuse and local TBIs. Following diffuse injury, functional ERP networks in injured groups showed hypo-connectivity compared to the sham group, and enhancement of connectivity compared to pre-injury. We achieved 82% accuracy in the prediction of TBI from the functional connectivity networks of ERPs. Auditory ERPs provide a clinically adoptable method that provides fast, mobile and objective indications of TBI. This work has applications to sports-related concussions and strategies for early TBI detection, prevention and reduction of severity.

Author contributions

All authors had full access to all the data in the study and take responsibility for the integrity of the data and the accuracy of the data analysis. Study concept and design: LA, SSM. Acquisition of data: LA, CS, IL. Analysis and interpretation of data: LA, IL, SSM. Drafting of the manuscript: LA, SSM. Critical revision of the manuscript for important intellectual content: LA, SSM. Statistical analysis: LA. Obtained funding: SSM. Administrative, technical, and material support: SSM. Study supervision: SSM.

Acknowledgements

The authors acknowledge Dr. Shanti Tummala, Dr. Todd Kilbaugh, Ross Plyler, Jennifer Shotto, Madeline Stolow, Dr. Dennis Molfese, Carlie Badder, Amy Kronyn, Dr. Yale Cohen and Rewati Kulkarni for their technical assistance with data acquisition and helpful discussions. This study was made possible by the support of the NIH U01 NS06945, NIH R01 NS097549, and the Stephenson Fellow and Fontaine Fellow funds.

Appendix A. Supplementary data

Supplementary data to this article can be found online at https://doi.org/10.1016/j.clinbiomech.2018.05.013.

References

Andrews, R.J., Knight, R.T., Kirby, R.P., 1990. Evoked potential mapping of auditory and somatosensory cortices in the miniature swine. Neurosci. Lett. 114 (1), 27–31.
Arnfred, S.M., Lind, N.M., Gjedde, A., Hansen, A.K., 2004. Scalp recordings of mid-latency AEP and auditory gating in the Göttingen minipig: a new animal model in information processing research. Int. J. Psychophysiol. 52 (3), 267–275. http://dx.doi.org/10.1016/j.ijpsycho.2003.11.002.
Atlan, L.S., Smith, C., Margulies, S.S., 2017. Improved prediction of direction-dependent, acute axonal injury in piglets. J. Neurosci. Res. http://dx.doi.org/10.1002/jnr.24108.
Barachant, A., Bonnet, S., Congedo, M., Jutten, C., 2012. Multiclass brain–computer interface classification by Riemannian geometry. IEEE Trans. Biomed. Eng. 59 (4), 920–928.
Browne, K.D., Chen, X.-H., Meaney, D.F., Smith, D.H., 2011. Mild traumatic brain injury and diffuse axonal injury in swine. J. Neurotrauma 28 (9), 1747–1755.
Buckley, N.M., 1986. Maturation of circulatory system in three mammalian models of human development. Comp. Biochem. Physiol. A Physiol. 83 (1), 1–7. http://dx.doi.org/10.1016/0300-9629(86)90080-0.
Davis, G.A., Anderson, V., Babl, F.E., Gioia, G.A., Giza, C.C., Meehan, W., ... Zemek, R., 2017. What is the difference in concussion management in children as compared with adults? A systematic review. Br. J. Sports Med. 51 (12), 949–957. http://dx.doi.org/10.1136/bjsports-2016-097415.
De Beaumont, L., Brisson, B., Lassonde, M., Jolicoeur, P., 2007. Long-term electrophysiological changes in athletes with a history of multiple concussions. Brain Inj. 21 (6), 631–644. http://dx.doi.org/10.1080/02699050701426931.
Dennis, E.L., Ellis, M.U., Marion, S.D., Jin, Y., Moran, L., Olsen, A., ... Asarnow, R.F., 2015. Callosal function in pediatric traumatic brain injury linked to disrupted white matter integrity. J. Neurosci. 35 (28), 10202–10211. http://dx.doi.org/10.1523/JNEUROSCI.1595-15.2015.
Dickerson, J.W.T., Dobbing, J., 1967. Prenatal and postnatal growth and development of the central nervous system of the pig. Proc. R. Soc. Lond. B Biol. Sci. 166 (1005), 384–395. http://dx.doi.org/10.1098/rspb.1967.0002.
Duhaime, A.C., 1998. Age-specific therapy for traumatic injury of the immature brain:

experimental approaches. Pathophysiology 5, 236. http://dx.doi.org/10.1016/S0928-4680(98)81216-9.
Duhaime, A.-C., Gennarelli, T.A., Thibault, L.E., Bruce, D.A., Margulies, S.S., Wiser, R., 1987. The shaken baby syndrome: a clinical, pathological, and biomechanical study.
Dundon, N.M., Dockree, S.P., Buckley, V., Merriman, N., Carton, M., Clarke, S., ... Dockree, P.M., 2015. Impaired auditory selective attention ameliorated by cognitive training with graded exposure to noise in patients with traumatic brain injury. Neuropsychologia 75, 74–87. http://dx.doi.org/10.1016/j.neuropsychologia.2015.05.012.
Espy, K.A., Molfese, D.L., Molfese, V.J., Modglin, A., 2004. Development of auditory event-related potentials in young children and relations to word-level reading abilities at age 8 years. Ann. Dyslexia 54 (1), 9–38.
Eucker, S.A., Smith, C., Ralston, J., Friess, S.H., Margulies, S.S., 2011. Physiological and histopathological responses following closed rotational head injury depend on direction of head motion. Exp. Neurol. 227 (1), 79–88. http://dx.doi.org/10.1016/j.expneurol.2010.09.015.
Faul, M., Xu, L., Wald, M., Coronado, V., 2010. Traumatic brain injury in the United States: emergency department visits, hospitalizations and deaths 2002–2006. (Centers for Disease Control and Prevention, National Center for Injury Prevention and Control, 2010).
Gao, X., 2008. Nonparametric multiple comparison procedures for unbalanced one-way factorial designs. J. Stat. Plan. Inference 138, 2574–2591. Retrieved from. https://docslide.com.br/documents/nonparametric-multiple-comparison-procedures-for-unbalanced-one-way-factorial.html.
Gennarelli, T.A., Thibault, L.E., Adams, J.H., Graham, D.I., Thompson, C.J., Marcincin, R.P., 1982. Diffuse axonal injury and traumatic coma in the primate. Ann. Neurol. 12 (6), 564–574.
Gosselin, N., Thériault, M., Leclerc, S., Montplaisir, J., Lassonde, M., 2006. Neurophysiological anomalies in symptomatic and asymptomatic concussed athletes. Neurosurgery 58 (6), 1151–1161. http://dx.doi.org/10.1227/01.NEU.0000215953.44097.FA.
Harris, N.G., Verley, D.R., Gutman, B.A., Thompson, P.M., Yeh, H.J., Brown, J.A., 2016. Disconnection and hyper-connectivity underlie reorganization after TBI: a rodent functional connectomic analysis. Exp. Neurol. 277, 124–138. http://dx.doi.org/10.1016/j.expneurol.2015.12.020.
Heisz, J.J., McIntosh, A.R., 2013. Applications of EEG neuroimaging data: event-related potentials, spectral power, and multiscale entropy. J. Vis. Exp. 76. http://dx.doi.org/10.3791/50131.
Hillary, F.G., Rajtmajer, S.M., Roman, C.A., Medaglia, J.D., Slocomb-Dluzen, J.E., Calhoun, V.D., ... Wylie, G.R., 2014. The rich get richer: brain injury elicits hyperconnectivity in core subnetworks. PLoS One 9 (8), e104021. http://dx.doi.org/10.1371/journal.pone.0104021.
Hillary, F.G., Roman, C.A., Venkatesan, U., Rajtmajer, S.M., Bajo, R., Castellanos, N.D., 2015. Hyperconnectivity is a fundamental response to neurological disruption. Neuropsychology 29 (1), 59–75. http://dx.doi.org/10.1037/neu0000110.
Honey, C.J., Sporns, O., Cammoun, L., Gigandet, X., Thiran, J.P., Meuli, R., Hagmann, P., 2009. Predicting human resting-state functional connectivity from structural connectivity. Proc. Natl. Acad. Sci. 106 (6), 2035–2040. http://dx.doi.org/10.1073/pnas.0811168106.
Ibrahim, N.G., Ralston, J., Smith, C., Margulies, S.S., 2010. Physiological and pathological responses to head rotations in toddler piglets. J. Neurotrauma 27 (6), 1021–1035. http://dx.doi.org/10.1089/neu.2009.1212.
Kraus, N., Thompson, E.C., Krizman, J., Cook, K., White-Schwoch, T., LaBella, C.R., 2016. Auditory biological marker of concussion in children. Sci. Rep. 6, srep39009. http://dx.doi.org/10.1038/srep39009.
Kumar, S., Rao, S.L., Chandramouli, B.A., Pillai, S.V., 2009. Reduction of functional brain connectivity in mild traumatic brain injury during working memory. J. Neurotrauma 26 (5), 665–675. http://dx.doi.org/10.1089/neu.2008.0644.
Margulies, S.S., Kilbaugh, T., Sullivan, S., Smith, C., Propert, K., Byro, M., ... Duhaime, A.-C., 2015. Establishing a clinically relevant large animal model platform for TBI therapy development. Brain Pathol. 25 (3), 289–303. http://dx.doi.org/10.1111/bpa.12247.
Martoft, L., Jensen, E.W., Rodriguez, B.E., Jørgensen, P.F., Forslid, A., Pedersen, H.D., 2001. Middle-latency auditory evoked potentials during induction of thiopentone anaesthesia in pigs. Lab. Anim. 35 (4), 353–363.
Mayer, A.R., Mannell, M.V., Ling, J., Gasparovic, C., Yeo, R.A., 2011. Functional connectivity in mild traumatic brain injury. Hum. Brain Mapp. 32 (11), 1825–1835. http://dx.doi.org/10.1002/hbm.21151.
Mazzini, L., Zaccala, M., Gareri, F., Giordano, A., Angelino, E., 2001. Long-latency auditory-evoked potentials in severe traumatic brain injury. Arch. Phys. Med. Rehabil. 82 (1), 57–65. http://dx.doi.org/10.1053/apmr.2001.18076.
Mishra, A.M., Bai, X., Sanganahalli, B.G., Waxman, S.G., Shatillo, O., Grohn, O., ... Blumenfeld, H., 2014. Decreased resting functional connectivity after traumatic brain injury in the rat. PLoS One 9 (4), e95280. http://dx.doi.org/10.1371/journal.pone.0095280.
Pedregosa, F., Varoquaux, G., Gramfort, A., Michel, V., Thirion, B., Grisel, O., ... Duchesnay, É., 2011. Scikit-learn: machine learning in python. J. Mach. Learn. Res. 12 (Oct), 2825–2830.
R Core Team, 2017. R: A language and environment for statistical computing. In: R Foundation for Statistical Computing, Vienna, Austria, Retrieved from. https://www.R-project.org/.
Rigon, A., Duff, M.C., McAuley, E., Kramer, A.F., Voss, M.W., 2015. Is traumatic brain injury associated with reduced inter-hemispheric functional connectivity? A study of large-scale resting state networks following traumatic brain injury. J. Neurotrauma 33 (11), 977–989. http://dx.doi.org/10.1089/neu.2014.3847.
Rivet, B., 2009. xDAWN algorithm to enhance evoked potentials: application to brain computer interface. IEEE Trans. Biomed. Eng. 56 (8), 2035–2043. Retrieved from. http://www.gipsa-lab.grenoble-inp.fr/~bertrand.rivet/references/Rivet2009a.pdf.
Rivet, B., 2011. Theoretical analysis of xDAWN algorithm: application to an efficient sensor selection in a P300 BCI. In: Signal Processing Conference, 2011 19th European, pp. 1382–1386.
Rivet, B., Souloumiac, A., 2007. Subspace estimation approach to P300 detection and application to brain-computer interface. In: Conference Proceedings: … Annual International Conference of the IEEE Engineering in Medicine and Biology Society. IEEE Engineering in Medicine and Biology Society. Annual Conference, 2007pp. 5071–5074. http://dx.doi.org/10.1109/IEMBS.2007.4353480.
Rogers, J.M., Fox, A.M., Donnelly, J., 2015. Impaired practice effects following mild traumatic brain injury: an event-related potential investigation. Brain Inj. 29 (3), 343–351. http://dx.doi.org/10.3109/02699052.2014.976273.
Sharp, D.J., Beckmann, C.F., Greenwood, R., Kinnunen, K.M., Bonnelle, V., De Boissezon, X., ... Leech, R., 2011. Default mode network functional and structural connectivity after traumatic brain injury. Brain J. Neurol. 134 (Pt 8), 2233–2247. http://dx.doi.org/10.1093/brain/awr175.
Smith, D.H., Meaney, D.F., Shull, W.H., 2003. Diffuse axonal injury in head trauma. J. Head Trauma Rehabil. 18 (4), 307–316.
Sponheim, S.R., McGuire, K.A., Kang, S.S., Davenport, N.D., Aviyente, S., Bernat, E.M., Lim, K.O., 2011. Evidence of disrupted functional connectivity in the brain after combat-related blast injury. NeuroImage 54 (Suppl 1), S21–S29. http://dx.doi.org/10.1016/j.neuroimage.2010.09.007.
Stevens, M.C., Lovejoy, D., Kim, J., Oakes, H., Kureshi, I., Witt, S.T., 2012. Multiple resting state network functional connectivity abnormalities in mild traumatic brain injury. Brain Imaging Behav. 6 (2), 293–318. http://dx.doi.org/10.1007/s11682-012-9157-4.
Sullivan, S., Eucker, S.A., Gabrieli, D., Bradfield, C., Coats, B., Maltese, M.R., Margulies, S.S., 2015. White matter tract-oriented deformation predicts traumatic axonal brain injury and reveals rotational direction-specific vulnerabilities. Biomech. Model. Mechanobiol. 14 (4), 877–896. http://dx.doi.org/10.1007/s10237-014-0643-z.
Weeks, D., Sullivan, S., Kilbaugh, T., Smith, C., Margulies, S.S., 2014. Influences of developmental age on the resolution of diffuse traumatic intracranial hemorrhage and axonal injury. J. Neurotrauma 31 (2), 206–214.
Yi, H., Guo, W., Chen, W., Chen, L., Ye, J., Yang, S., 2016. Miniature pigs: a large animal model of cochlear implantation. Am. J. Transl. Res. 8 (12), 5494–5502.